

Corrosion of HIPed β -Si_{6-z}Al_zO_zN_{8-z} ($z = 0, 1, 2, 3$) ceramics by NaCl vapor

Shiro Shimada*, Takafumi Okuyama, Hajime Kiyono, Junichi Takahashi

Division of Materials Science and Engineering, Graduate School of Engineering, Hokkaido University, Sapporo 060-8628, Japan

Received 15 March 2002; accepted 7 October 2002

Abstract

Tests for the corrosion of β -Si_{6-z}Al_zO_zN_{8-z} ($z = 0, 1, 2, 3$) (β -Si₃N₄ and β -SiAlON) ceramics were carried out at 1300 °C for 3–24 h in NaCl vapor of various concentrations (1.67×10^{-2} , 3.33×10^{-2} , 5.0×10^{-2} g l⁻¹), which was carried by flowing Ar gas. The densified Si₃N₄ and SiAlON ceramics were fabricated by HIPing under N₂ of 150 MPa at 1700 °C. The corroded surface was observed by optical and scanning electron microscopy (OM and SEM). The phases produced during corrosion were identified by X-ray diffraction. The thickness of the corroded scale was determined by cross sectional SEM observation. The Si₃N₄ ceramics were hardly corroded by NaCl vapor, while the $z = 1$ and 2 SiAlONs were slightly corroded with the formation of bubbles on the surface; the $z = 3$ ceramics were severely corroded with the formation of Al₂O₃ needle crystals and fine mullite crystals, depending on the NaCl vapor concentration. Quantitative X-ray microanalysis showed that 2 at.% Na is contained in all the scales of the SiAlONs. The severe corrosion of the $z = 3$ SiAlON was explained on the basis of the kinetic results for the thickness of the scale.

© 2003 Elsevier Science Ltd. All rights reserved.

Keywords: Corrosion; Kinetics; NaCl vapor; Sialons

1. Introduction

SiAlONs occur with various compositions and structures, such as α -, β -, O- and X-SiAlON and mixtures of these phases,^{1,2} which have found applications as high temperature engineering ceramics, cutting tools, and abrasive materials.¹ Of these, β -SiAlON is structurally related to β -Si₃N₄ and has the composition, Si_{6-z}Al_zO_zN_{8-z}, where z ranges from 0, corresponding to pure Si₃N₄, to ca. 4.3. There have been many reports regarding the corrosion of SiC and Si₃N₄ by molten Na₂CO₃ or Na₂SO₄-deposit or in an atmosphere containing Na/K vapor or chlorine gas at high temperatures > 900 °C.^{3–9} Jacobson has reviewed the corrosion of SiC induced by Na₂SO₄ deposit from both the kinetic and thermodynamic viewpoints.⁸

Similarly to Si₃N₄, SiAlONs are expected to be useful as materials resistant against oxidation/corrosion at high temperatures. Much attention has been paid to oxidation of α - and β -SiAlON by dry and wet O₂, including our previous studies,^{10–13} but few studies have

been reported on the corrosion of SiAlONs by alkaline molten salt or vapor, or chlorine gas except for an environment containing H₂S or Cl₂ gas.¹⁴ It is of value to investigate the corrosion of SiAlON ceramics by alkaline vapor at high temperatures > 800 °C and to compared this with the performance of Si₃N₄.

In our previous paper, F-containing SiAlONs have been prepared, for the first time, using AlF₃ or topaz as sources of fluorine by HIPing at 1500–1770 °C; these exhibited a high resistance against severe corrosion by NaCl vapor, due to the presence of F with its high electro-negativity.¹⁵ It is of interest to examine how other SiAlON ceramics are corroded by Na- or K-salt vapor, depending on the z value. The corrosion of SiAlONs by Na- or K-salt vapor becomes complex, when oxidation is simultaneously involved. The present paper describes the corrosion of β -SiAlON ceramics with $z = 0, 1, 2, 3$ ($z = 0$ corresponds to Si₃N₄) in NaCl vapor carried by Ar gas at 1300 °C. Since the $z = 3$ β -SiAlON was severely corroded by NaCl vapors at this temperature, the mechanism of corrosion was discussed for this composition from kinetic considerations and from the microstructural observation of the scales. It is well known that high temperature corrosion is strongly

* Corresponding author. Fax: +81-11-706-6576.

E-mail address: shimashi@eng.hokudai.ac.jp (S. Shimada).

affected by the volume fractions and compositions of the grain boundary phases formed with sintering additives. For simplification, dense Si_3N_4 and SiAlON ceramics fabricated by HIPing without any additives were used for these corrosion studies.

2. Experimental procedure

The $\alpha\text{-Si}_3\text{N}_4$ and $\beta\text{-sialon}$ powders ($z = 1, 2, 3$) were purchased from Ube Industries, Ltd. According to the manufacturer, the impurities present in the $\alpha\text{-Si}_3\text{N}_4$ are O (<2.0 wt.%), C (<0.2 wt.%), Cl (<100 ppm) and Fe (<100 ppm). The impurities present in the $\beta\text{-sialon}$ powders were not reported by the supplier. The nominal z value of 1, 2 and 3 were confirmed to be 1.0, 2.1 and 3.0, respectively, by powder XRD measurements of the unit cell parameters.^{1,15} Pellets of 12 mm diameter \times 5 mm height were made from the starting powder by cold isostatic pressing at 100 MPa; these were then embedded in fine BN powders and encapsulated by sealing in a glass tube. The pellet was sintered by HIPing under a N_2 gas pressure of 150 MPa at 1700 °C for 2 h. After HIPing, the pellet was powdered for the phase identification by X-ray diffraction (XRD). The density of the ceramics was measured by the Archimedes method using water.

The corrosion of the HIPed Si_3N_4 and SiAlON ceramics was conducted in the experimental apparatus shown in Fig. 1. The corrosion setup consists of two furnaces, one for the corrosion sample and the other for the generation of NaCl vapor. Each specimen of HIPed ceramic (approximately 5 mm \times 5 mm \times 1 mm) and a loosely packed NaCl compact were placed on an alumina boat in the main and auxiliary furnace, respectively. Before corrosion, the system was evacuated and then replaced with Ar gas. The NaCl compact was heated at 860 °C, at which the generated vapor was carried to the corrosion zone by flowing Ar gas; the oxygen and water vapors contained in the Ar were reported to approximately be a few and 3 Pa, respectively, by the supplier. Corrosion was carried out isothermally at 1300 °C for 3–24 h at a NaCl concentration

of 1.67×10^{-2} , 3.33×10^{-2} and $5.0 \times 10^{-2} \text{ g l}^{-1}$ (within errors of less than 10%), which was changed by the rate of flowing Ar gas (0.05 l min^{-1}). Ar gas containing the NaCl vapor was exhausted through liquid paraffin to air.

The phases formed on the surface of the as-corroded specimen were identified by XRD, using the reflection method. The surface of the as-corroded specimen was observed by optical and scanning electron microscopy (OM and SEM). The corroded specimen was cut and polished for cross-sectional SEM observation to examine the corroded scale and to determine its thickness. Wavelength-dispersive spectroscopy, coupled with X-ray microanalysis (WDS-XMA) was conducted to determine quantitatively the atomic concentration of Na, Si, Al, O, N, and Cl in the corroded scale.

3. Results and discussion

After HIPing, the z value of the $\beta\text{-SiAlON}$ was determined to be almost the same as that of the starting powder, but $\alpha\text{-Si}_3\text{N}_4$ was changed to $\beta\text{-Si}_3\text{N}_4$ with a trace of $\text{Si}_2\text{N}_2\text{O}$. The density of the Si_3N_4 and $\beta\text{-SiAlON}$ ($z = 1, 2, 3$) ceramics was determined to be 95, 94, 97, 99%, respectively. Quantitative XMA analysis was performed to determine the concentrations of Si, N, Al, O, and the impurities (K, Na, Fe, Mg, or Ca) in the polished surface of the HIPed ceramics. It was found that no segregation of any specific element occurs at the grain boundaries. Fig. 2 shows the etched surface of the HIPed SiAlON s ceramics prepared by using a 40% HF solution. The surface of the $z = 1$ SiAlON exhibits many etch pits, probably formed by the removal of glass phases, and at $z = 2$, the number and size of pits are decreased. The $z = 3$ ceramics show the least pits, in accord with the high density (99%) of the material.

When corroded in flowing NaCl vapor with a concentration of $3.33 \times 10^{-2} \text{ g l}^{-1}$ at 1300 °C for 6 h, the Si_3N_4 and SiAlON s ceramics showed different corrosion behaviors, as seen by OM observation (Fig. 3). There is no apparent change on the surface of the Si_3N_4 ceramics; the surface showed little change even after being

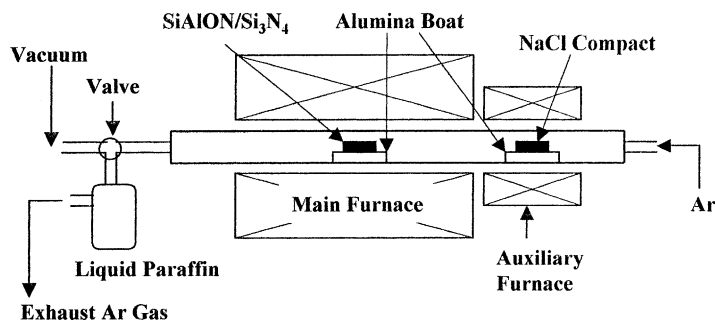


Fig. 1. Schematic apparatus for corrosion of Si_3N_4 and SiAlON s by NaCl vapor.

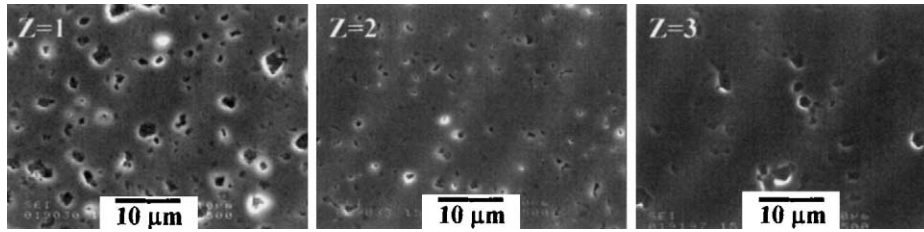


Fig. 2. Optical microscopy of etched surface of HIPed SiAlONs.

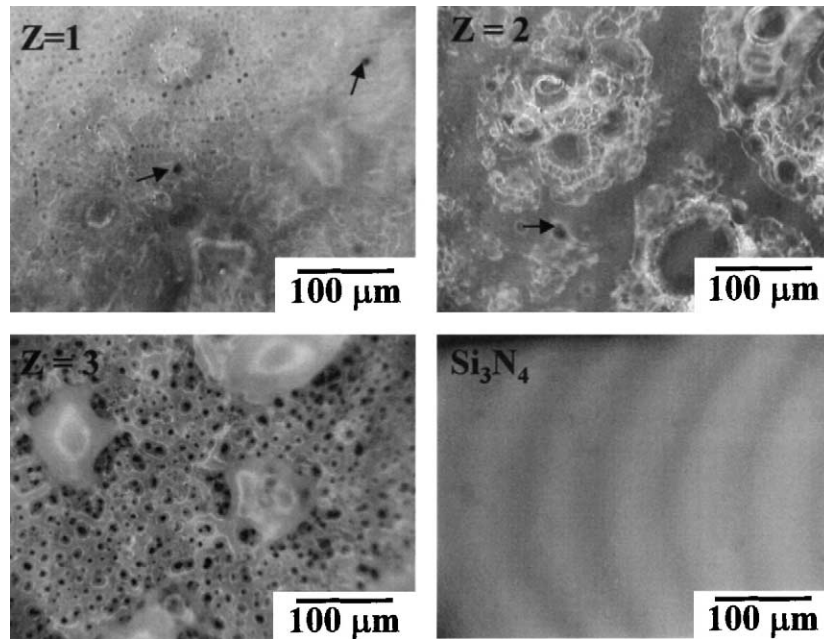


Fig. 3. Corroded surface of Si_3N_4 and SiAlONs by NaCl vapor. Corrosion; 1300 °C, 6 h, NaCl concentration $3.33 \times 10^{-2} \text{ g l}^{-1}$.

exposed for extended times (to 24 h). The $z=1$ and 2 SiAlONs show the presence of some transparent bubbles of several tens of microns in size with small etch pits (see arrows) on the corroded surface, their number and size increasing at $z=2$ and also increasing with time. For example, the bubbles eventually grow or swell up to large ones of several hundred microns in size. At $z=3$, many pits and bubbles of about 10 and 100 μm in size, respectively, are formed on the surface at relatively early times (<6 h), the bubbles being merged into each other and changing to big fragile mounds of several hundred μm in size. It was found that the SiAlONs are corroded with the formation of bubbles on the surface, severely at $z=3$, which is associated with the interaction between the evolving N_2 gas and the viscous melts.

Fig. 4 shows the XRD patterns of the surface of the Si_3N_4 and the $z=1$, 2, and 3 SiAlONs corroded under the same condition as in Fig. 3. On the corroded Si_3N_4 , no peaks appear except for Si_3N_4 ; a very small amount of SiO_2 (cristobalite) was detected at times > 12 h. At $z=1$ and 2, a small peak of SiO_2 appears; the SiAlON peaks slightly decrease at $z=2$. At $z=3$, the peaks of mullite with a small SiO_2 peak are observed, with the

Table 1
Quantitative analysis of scales produced form SiAlONs

z value	Si	Al	O	Na	N	Cl
z=1	25	5	68	2	0	0
z=2	□	20	10	68	2	0
z=3	□	15	15	68	2	0

SiAlON peaks greatly decreased. Table 1 shows the quantitative XMA analysis in the corroded scales of the SiAlONs, showing that all the scales contain the elements of Na, Si, Al, and O, but neither N nor Cl. The composition ratio of Al to Si in the scales is 1:1, 2:1, and 5:1, in a good agreement with that of the $z=1$, 2, and 3 SiAlONs, respectively. In reference to the ternary phase diagram of $\text{SiO}_2\text{--Al}_2\text{O}_3\text{--Na}_2\text{O}$,¹⁶ the scales containing 2 at.% Na are predicted to form sodium aluminum silicate, SiO_2 , and mullite; sodium aluminum silicate exists as a glassy phase at the corrosion temperature of 1300 °C. This prediction fairly agrees with the corrosion results that SiO_2 forms in the corroded scales at $z=1$ and 2, and SiO_2 and mullite at $z=3$. The absence of

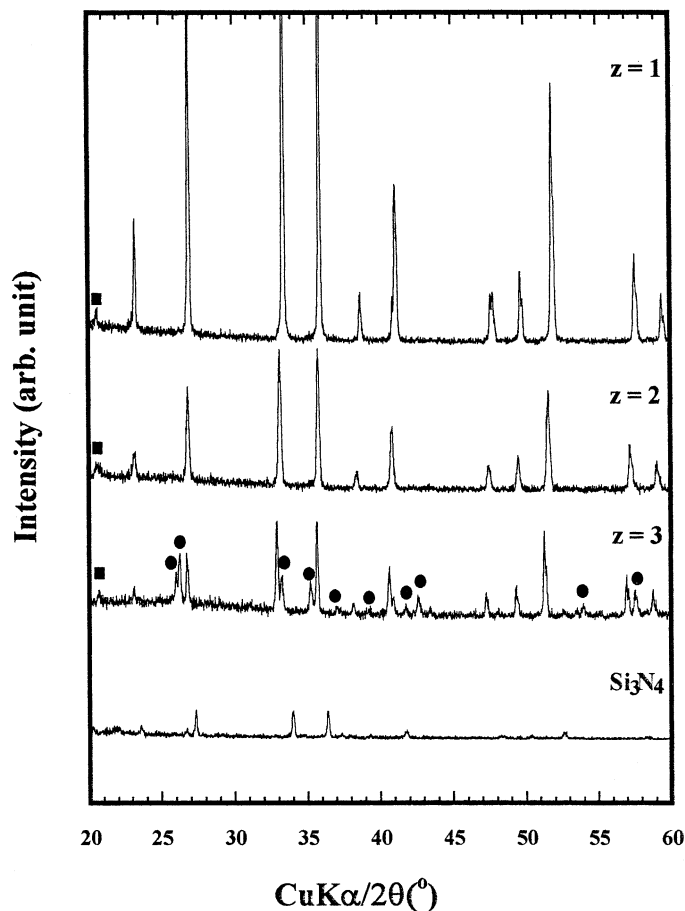


Fig. 4. XRD of corroded surface of Si_3N_4 and SiAlONs by NaCl vapor. Corrosion was the same as in Fig. 3. ● mullite, ■ SiO_2 (cristobalite).

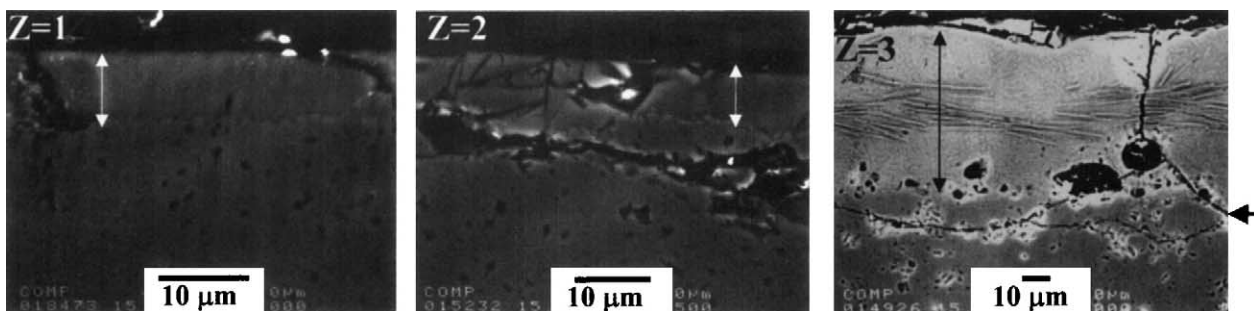


Fig. 5. Cross-sectional observation of corroded SiAlONs by SEM. Corrosion was the same as in Fig. 3.

mullite peaks at $z=1$ and 2 on XRD is due to the insufficient amount of Al component in the SiAlONs to form detectable quantities of mullite.

Cross sections of the corroded SiAlONs were observed by SEM (Fig. 5), which shows that the scale formed at $z=1$ and 2 (inserted as an arrow) is about $10\ \mu\text{m}$ thick with large cracks oblique or parallel to the surface. The $z=3$ SiAlON is largely corroded, with a scale of about $60\ \mu\text{m}$ thickness containing many large pores and continuous cracks along the boundary (see side arrow) and the cracked surface. Needle like crystals are seen to lie in the middle of the scale. In the case of the Si_3N_4 , a distinct corroded scale was not observed.

Since the $z=3$ SiAlON was severely corroded by NaCl vapor, the corrosion is discussed in more detail for the material. Fig. 6 shows the XRD patterns of the corroded surface of the SiAlON produced at various concentrations of NaCl vapor (1.67×10^{-2} , 3.33×10^{-2} , $5.0 \times 10^{-2}\ \text{g l}^{-1}$) for 6 h. The mullite peaks with a trace of SiO_2 appear at 1.67×10^{-2} and $3.33 \times 10^{-2}\ \text{g l}^{-1}$. The SiAlON peaks decrease greatly with increasing NaCl concentration and eventually disappear at $5.0 \times 10^{-2}\ \text{g l}^{-1}$. A broad signal is seen at the diffraction angles of 20° – 30° , probably due to the presence of glassy phase. The corrosion of the $z=3$ SiAlON with time also was examined at a fixed NaCl concentration

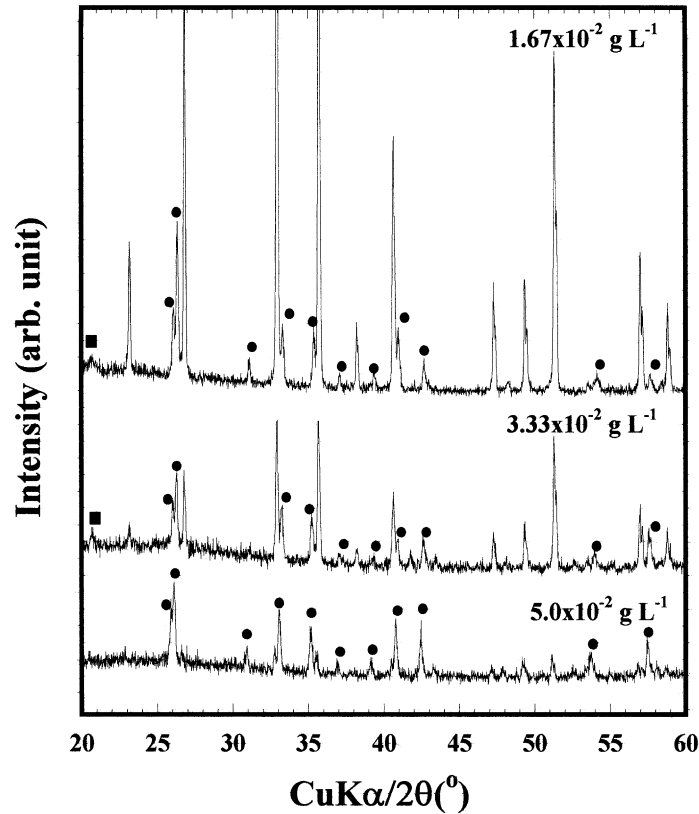


Fig. 6. XRD of corroded surface of $z=3$ SiAlON by NaCl vapor with a concentration of 1.67×10^{-2} , 3.33×10^{-2} , and $5.0 \times 10^{-2} \text{ g L}^{-1}$. Corrosion; 1300°C , 6 h. ● mullite, ■ SiO_2 (cristobalite).

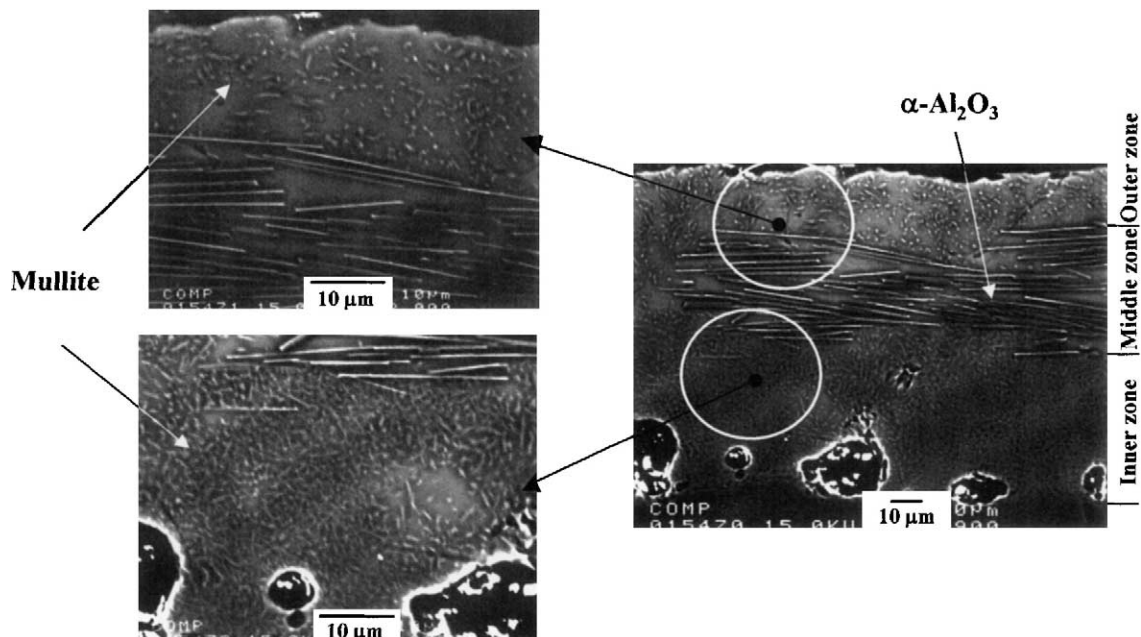


Fig. 7. Cross-sectional observation of corroded $z=3$ SiAlON by SEM. Corrosion; 1300°C , 12 h, NaCl concentration $3.33 \times 10^{-2} \text{ g L}^{-1}$.

($3.33 \times 10^{-2} \text{ g L}^{-1}$). A considerable amount of mullite was already formed after 3 h and the signals were then unchanged with time. The SiAlON signals gradually decreased with time and finally disappeared at 24 h.

Cross sectional SEM observation of the corroded $z=3$ SiAlON scale produced at a concentration of $3.33 \times 10^{-2} \text{ g L}^{-1}$ for 12 h is shown in Fig. 7. The scale reaches $80 \mu\text{m}$ thick and is divided into three zones. The inner zone contains randomly oriented fine needle-like

particles 2–5 μm long with large pores ranging from 5 to 20 μm near the boundary. The middle zone of 25 μm thickness contains long needle crystals of 10–50 μm lying almost parallel to the surface, with a small amount of the fine crystals. The outer zone contains fine needle-like crystals in lower concentration than in the inner zone. Quantitative XMA analysis showed that the long needle and fine crystals in the middle and inner/outer zones are Al_2O_3 and mullite, respectively. The Al_2O_3 needles tend to grow with higher aspect ratio at extended times (to 24 h). It seems that glassy phases predominate except for the Al_2O_3 and mullite crystals.

The scale thickness of the corroded $z = 3$ SiAlON was determined at the NaCl concentrations of 1.67×10^{-2} , 3.33×10^{-2} , $5.0 \times 10^{-2} \text{ g l}^{-1}$ by cross-sectional SEM observation and plotted as a function of $t^{1/2}$ (Fig. 8). The straight lines at the three concentrations meet at the time of 1 h on the abscissa, suggesting that the corrosion occurs by a diffusion limited process after the induction time (1 h). The time 1 h is that needed for the initiation of the corrosion of $z = 3$ SiAlON. The corrosion rate is increased with increasing NaCl concentration and the corroded layer reaches 260 μm thickness after 24 h at $5.0 \times 10^{-2} \text{ g l}^{-1}$.

As described above, the scales contained the elements Si, Al, O, and Na distributed uniformly in the scale, but neither N nor Cl. The four elements Si, Al, O, and Na contribute to form SiO_2 , Al_2O_3 , mullite, and sodium

aluminum silicate as a glassy phase, as seen in Figs. 4, 6, and 7. Thermodynamic considerations suggest that the reaction of SiAlON with NaCl does not occur. Accordingly, the formation of SiO_2 , mullite, and sodium aluminum silicate glass is strongly associated with the oxidation of SiAlON. A 10 mm sized graphite block was placed in the main furnace in flowing Ar gas at 1300 °C for 12 h, giving 5 wt.% weight loss. A piece of the SiAlON was also placed under the same condition, giving no apparent weight change, but a trace of mullite and cristobalite on XRD. These results suggest that a trace of O_2 and/or H_2O contained in the Ar gas acts as oxidant for SiAlONs. A small amount of white powder was collected at a low temperature region of the system down stream after the corrosion. The presence of Si in the powder was confirmed by EDX, implying that the Si component of SiAlON is transported as SiCl_4 gas by flowing Ar gas to the lower temperature region. It is assumed that the oxidation of SiAlON with a trace of O_2 and/or H_2O in Ar gas occurs to give SiO_2 and mullite.^{12,13} A large amount of SiO_2 is reacted with NaCl to give $\text{Na}_2\text{O} + \text{gaseous SiCl}_4$.

Jacobson et al. have reported that Na_2O reacts with mullite to form albite ($\text{Na}_2\text{O} \cdot \text{Al}_2\text{O}_3 \cdot \text{SiO}_2$) and Al_2O_3 in a triangle region of the mullite–albite–alumina system.¹⁷ It seems that for corrosion of the $z = 3$ SiAlON, the oxidation of SiAlON with a trace of $\text{O}_2/\text{H}_2\text{O}$ initiates to give SiO_2 and mullite, followed by the reaction of Na_2O with mullite which produces the sodium aluminum silicate melt and alumina at 1300 °C. Al_2O_3 needles were formed in the middle zone, around which fine mullite crystals are rarely seen (Fig. 7), supporting this idea that the reaction of mullite with Na_2O gives Al_2O_3 and sodium aluminum silicate. At present, it is not explained why this reaction occurs in the middle zone. It is likely that the Al_2O_3 is encouraged to grow as needle crystals in the sodium aluminum silicate melt. It is concluded that the $z = 3$ SiAlONs are severely corroded by NaCl vapor after the induction time (1 h), which is needed for the oxidation of SiAlONs by a trace of $\text{O}_2/\text{H}_2\text{O}$ contained in the Ar to make SiO_2 and mullite. Since large bubbles are formed at the boundary, it seems that the out-diffusion of N_2 gas produced by oxidation of SiAlON occurs during the corrosion.

4. Conclusion

Densified Si_3N_4 and $z = 1, 2, 3$ SiAlON ceramics were corroded at 1300 °C for 3–24 h in NaCl vapor with a concentration of 1.67×10^{-2} , 3.33×10^{-2} , $5.0 \times 10^{-2} \text{ g l}^{-1}$ carried by flowing Ar gas. The Si_3N_4 ceramics were hardly corroded, with no apparent change in the surface condition. Some 2 at.% Na was found to be contained in all the scales of the SiAlONs. The $z = 1$ and 2 SiAlONs were slightly corroded with the formation of bubbles and

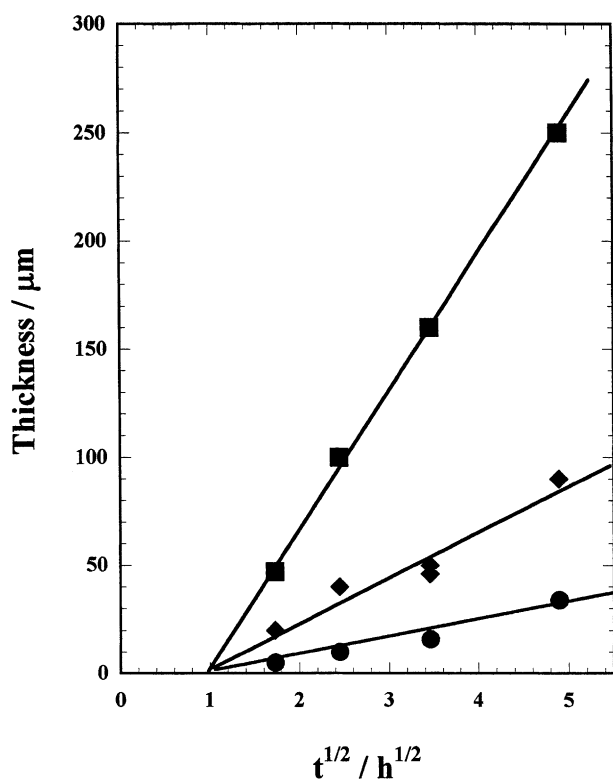


Fig. 8. Plots of scale thickness vs. $t^{1/2}$ for corrosion of $z = 3$ SiAlON at 1300 °C. ● $1.67 \times 10^{-2} \text{ g l}^{-1}$, ◆ $3.33 \times 10^{-2} \text{ g l}^{-1}$, ■ $5.0 \times 10^{-2} \text{ g l}^{-1}$.

SiO₂ (cristobalite) on the surface; the scale was about 10 μm thick. The $z=3$ ceramics were severely corroded with the formation of many large bubbles and etch pits on the surface. The corroded scale contained needle-formed Al₂O₃ crystals and fine mullite crystals with sodium aluminum silicate glass and reached 260 μm thick at a concentration of $5.0 \times 10^{-2} \text{ g l}^{-1}$ for 24 h. Parabolic growth of the scale at $z=3$ was found to occur, the rate increasing with increasing NaCl concentration. It was suggested that the corrosion of the $z=3$ SiAlONs was initiated by oxidation with a trace of O₂ and/or H₂O contained in the Ar gas. An induction time of 1 h was needed for the initiation, after which time the corrosion proceeds with the bubble formation from the out-diffusion of N₂ gas produced.

References

1. Ekstrom, T. and Nygren, M., SiAlON ceramics. *J. Am. Ceram. Soc.*, 1992, **75**, 259–276.
2. Riley, F. L., Silicon nitride and related materials. *J. Am. Ceram. Soc.*, 2000, **83**, 245–265.
3. McKee, D. W. and Chatterji, D., Corrosion of silicon carbide in gases and alkaline melts. *J. Am. Ceram. Soc.*, 1976, **59**, 441–444.
4. Jacobson, N. S., Kinetics and mechanism of corrosion of SiC by molten salts. *J. Am. Ceram. Soc.*, 1986, **69**, 74–82.
5. Jacobson, N. S. and Smialek, J. L., Corrosion pitting of SiC by molten salts. *J. Electrochem. Soc.*, 1986, **133**, 2615–2621.
6. Bourne, W. C. and Tressler, R. E., Molten salt degradation of Si₃N₄ ceramics. *Am. Ceram. Soc. Bull.*, 1980, **59**, 443–446.
7. Pareek, V. and Shores, D. A., Oxidation of SiC in environments containing K-salt vapor. *J. Am. Ceram. Soc.*, 1991, **74**, 556–563.
8. Jacobson, N. S., Corrosion of silicon-based ceramics in combustion environments. *J. Am. Ceram. Soc.*, 1993, **76**, 3–28.
9. Sun, T., Pickrell, G. R. and Brown, J. J. Jr., Corrosion kinetics of Si₃N₄ in dry air containing sodium nitrate vapors. *J. Am. Ceram. Soc.*, 1994, **77**, 3209–3214.
10. MacKenzie, K. D. J., Shimada, S. and Aoki, T., Thermal oxidation of carbothermal β-sialon powder: reaction sequence and kinetics. *J. Mater. Chem.*, 1997, **7**, 527–530.
11. Shimada, S., Aoki, T., Kiyono, H. and MacKenzie, K. J. D., Early-stage thermal oxidation of carbothermal β-sialon powder. *J. Am. Ceram. Soc.*, 1998, **81**, 266–268.
12. Kiyono, H. and Shimada, S., Kinetic and magic angle spinning-nuclear magnetic resonance studies of dry oxidation of beta-sialon powders. *J. Electrochem. Soc.*, 2001, **148**, B79–B85.
13. Kiyono, H. and Shimada, S., Kinetic and magic angle spinning-nuclear magnetic resonance studies of wet oxidation of beta-sialon powders. *J. Electrochem. Soc.*, 2001, **148**, B86–B91.
14. Ramesh, R., Pomeroy, M. J., Chu, H. and Datta, P. K., Effect of gaseous environment on the corrosion of β-sialon materials. *J. Eur. Ceram. Soc.*, 1995, **15**, 1007–1014.
15. Shimada, S., Tanaka, M., Kiyono, H. and MacKenzie, K. J. D., Microstructure and properties of various fluorine-containing SiAlON ceramics synthesized by HIPing. *J. Eur. Ceram. Soc.*, 2001, **21**, 2811–2819.
16. Levin, E. M., Robbins, C. R. and McMurdie, H. F., *Phase Diagrams for Ceramists*. American Ceramics Society, Columbus, OH, 1964 p. 181.
17. Jacobson, N. S., Lee, K. N. and Yoshio, T., Corrosion of mullite by molten salts. *J. Am. Ceram. Soc.*, 1996, **79**, 2161–2167.